BIOCHEMISTRY
including biophysical chemistry & molecular biology

Article

pubs.acs.org/biochemistry

Formation of Highly Ordered Multimers in G-Quadruplexes

Petra Tóthová, Petra Krafčíková, and Viktor Víglaský*

Department of Biochemistry, Institute of Chemistry, Faculty of Sciences, P. J. Šafárik University, 04001 Košice, Slovakia

Supporting Information

ABSTRACT: G-Rich DNA and RNA have a higher propensity to form G-quadruplex structures, but the presence of G-runs alone is not sufficient to prove that such sequences can form stable G-quadruplexes. While G-rich sequences are essential for G-quadruplex formation, not all G-rich sequences have the propensity to form G-quadruplex structures. In addition, monovalent metal ions, dehydrating agents, and loop sequences connecting the G-runs also play important roles in the topology of G-quadruplex folding. To date, no quantitative analysis of the CD spectra of G-quadruplexes in confrontation with the electrophoretic results has been performed. Therefore, in this study, we use information gained through the analysis of a series of well-known G-quadruplex-forming sequences to evaluate other less-studied sets of aptameric sequences. A simple and cost-effective methodology that can verify the formation of G-quadruplex motifs from oligomeric DNA sequences and a technique to determine the molecularity of these structures are also described. This methodology could be of great use in the prediction of G-quadruplex assembly, and the basic principles of our techniques can be extrapolated for any G-rich DNA sequences. This study also presents a model that can predict the multimerization of G-quadruplexes; the predictions offered by this model are shown to match the results obtained using circular dichroism.

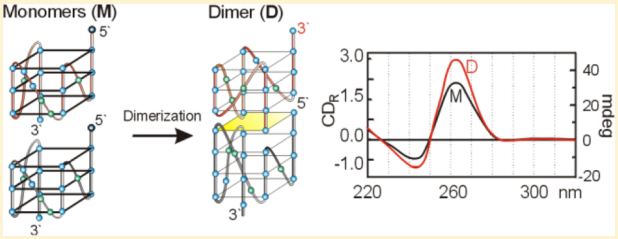

Short nucleic acids can fold into a wide variety of different structures, some of which display very high affinities for specific target molecules such as small ligands, proteins, nucleic acids, cells, and cell surface proteins; there is even some evidence of affinities for bacteria and viruses.[1,2] These structures, commonly known as aptamers, demonstrate levels of specificity that are comparable to and, in certain cases, even higher than those of antibodies. The stability of the complexes is characterized by the apparent dissociation constant, K_D, which usually lies within the range of 1−100 nM for aptamer−protein complexes. This level is similar to those of antibody−antigen complexes, although some aptamers bind to their target proteins with K_D values on the order of picomolar, for example, the K_D values of 100 pM for the PDGF-B DNA aptamer[3] and 49 pM for the VEGF RNA aptamer.[4]

Aptamers also possess a number of inherent advantages over antibodies; they exhibit low levels of toxicity and immunogenicity, while their small size allows for a simpler production process and greater potential for structural modification. The ability of aptamers to attach to various nanoparticles also makes them ideal candidates for use as carriers for a wide range of medical drugs; aptamers that are sensitive to, for example, cancer markers on the surface of cancer cells can provide targeted delivery of chemotherapeutic drugs or other agents.[1]

Aptamers also show a wide structural variability, and many different structural motifs have been identified in their structures. G-Quadruplex structures, four-stranded DNA structures that consist of planar arrays of four guanines (also known as a G-quartet) and intervening loops, are some of a number of structures that are capable of adopting aptamers. G-Quadruplex aptamers display several advantages over other folds; most G-quadruplexes are thermodynamically and chemically stable and exhibit greater resistance to various serum nucleases and an enhanced cellular uptake without the need for further chemical modification.[5,6] In addition to a number of other aptamers, aptameric G-quadruplexes have also shown great potential for the further development of nanodevices, such as basic components in microarrays, microfluidics, sandwich-type biosensors, and electrochemical assays.[7,8]

The length and orientation of the loops and the number of G-quartets are variable, indicating that G-quadruplexes may possess considerable structural diversity. This diversity suggests that G-quadruplex motifs have the potential to interact with many different structural motifs; for example, it has been suggested that G-quadruplexes tend to bind preferentially to the β-structures of proteins.[9] Moreover, G-quadruplexes show high levels of interaction with the cationic domain of protein due to the fact that the complexes have a negative charge density that is twice as strong as that of double helices.[10] This has led to suggestions that the presence of a G-quadruplex DNA motif would allow aptamers to recognize target proteins.[11]

An important concomitant effect of the folding process of G-rich oligonucleotides is their multimerization under certain conditions. If a short oligomeric DNA contains fewer Gs than the number necessary for G-quadruplex assembly, then it would be expected that at least two molecules would have to be associated to form the structure. However, multimerization is

Received: June 23, 2014
Revised: October 24, 2014
Published: October 27, 2014

   dx.doi.org/10.1021/bi500773c | *Biochemistry* 2014, 53, 7013−7027

Table 1. DNA Oligonucleotides Used in This Study

abbreviation	no. of nucleotides	ε_{257}[a]	sequence (5′ → 3′)	target	ref[b]
EA1−42	42	421.4	ATACCAGCTTATTCAATTTGAGGCGGGTGGGTGGGTTGAATA	ethanolamines	19
EA1	18	185.7	TGAGGCGGGTGGGTGGGT	ethanolamines	c
EA1D	17	172.2	TGGGCGGGTGGGTGGGT	ethanolamines	c
EA2	22	225.9	GCTGCGAGGCGGGTGGGTGGGA	ethanolamines	c
EA2D	21	212.4	GCTGCGGGCGGGTGGGTGGGA	ethanolamines	c
EA2a	18	190.9	CGAGGCGGGTGGGTGGGA	ethanolamines	c
EA2aD	17	177.3	CGGGCGGGTGGGTGGGA	ethanolamines	c
HCV	18	184.6	GGGCGTGGTGGGTGGGGT	hepatitis C virus	48
HIV-93del	16	178.3	GGGGTGGGAGGAGGGT	HIV integrase	34, 49
Hema	20	199.7	GGGGTCGGGCGGGCCGGGTG	hematoporphyrin IX	50, 51
Insu	24	253.4	GGTGGTGGGGGGGGTTGGTAGGGT	insulin	52
IonK	20	218.2	GGGTTAGGGTTAGGGTAGGG	potassium	53
Scle	17	177.4	TGGGGGGGTGGGTGGGT	sclerostin	54
STAT	16	158.2	GGGCGGGCGGGCGGGC	signal transducer and activator of transcript	55
TBA	15	149.3	GGTTGGTGTGGTTGG	thrombin	45, 56
TNF	18	182.4	GGTGGATGGCGCAGTCGG	tumor necrosis factor	35
apVEGF-D	20	201.2	TGGGGGTGGACGGGCCGGGT	vesicular endothelial growth factor	57
apVEGF	22	220.6	TGTGGGGGTGGACGGGCCGGGT	vesicular endothelial growth factor	57
HTR	21	225.4	GGGTTAGGGTTAGGGTTAGGG	telomeric repeats	18
bcl-2	23	269.0	GGGCGCGGGAGGAAGGGGGCGGG	promoter sequence	13, 14
c-myc	19	286.3	AGGGTGGGGAGGGTGGGGA	promoter sequence	16, 17
c-kit87	22	262.3	AGGGAGGGCGCTGGGAGGAGGG	promoter sequence	15
vegf	20	218.2	GGGGCGGGCCGGGGGCGGGG	promoter sequence	12

[a]Extinction coefficient at 257 nm in mM^{-1} cm^{-1}. [b]The core of G-quadruplex-forming sequences in the following articles. [c]The shortened version of sequences published by Cheng et al.[40] and Reinemann et al.[20]

observed in many oligonucleotides that demonstrate the potential to form intramolecular G-quadruplexes, and this process is thought to be thermodynamically driven. Multimeric forms are usually more stable than intramolecular conformers and also demonstrate potential for a wide range of technological applications.

The main aim of this study is to characterize the dependence of CD signal intensity on the specific topologies of a number of well-known G-quadruplexes and to use these findings to form some general rules that can be applied to G-quadruplex-forming sequences as a whole. The study will therefore focus initially on DNA sequences that are known to fold into G-quadruplexes: human telomeric repeats (HTR) and promoter sequences of c-kit87, c-myc, bcl-2, and vegf.[12−18] The conclusions obtained from the analysis of these initial G-quadruplex sequences will then be applied to a series of 18 less familiar aptameric DNA sequences that possess the potential to fold into G-quadruplex structures and are known to target a broad range of molecules. This study also introduces a model for the prediction of multimerization in various G-quadruplexes that is based on a comparison of circular dichroism (CD) spectra with a standard G-quadruplex. In this particular case, HTR is used as the standard G-quadruplex for three layered G-quadruplex structures. Thermal differential spectra (TDS), UV spectra, and gel electrophoresis data were also used to supplement CD studies.

Interestingly, many of these G-complexes are unstable in the presence of sodium without potassium ions, but research into these molecules to date has been conducted in the absence of potassium ions. The analysis of these complexes in this study was performed under conditions that included both sodium and potassium and would therefore be useful in determining the conditions in which G-quadruplexes remain stable. This ability is crucial in allowing the aptamers to recognize a specific target molecule and would be of particular use in the development of aptamer-based biosensors and nanodevices.

The experimental approaches that are applied here may be valuable in the study of unknown sequences and in confirming both the formation of G-quadruplex structures and their structural features such as strand orientation and multimerization.

MATERIALS AND METHODS

All chemicals and reagents were obtained from commercial sources. DNA oligonucleotides were obtained from Metabion (Table 1). In this study, the derivatives of a series of previously described EA aptamers were analyzed.[19] EA1−42 is a shortened version of EA#14.3,[20] but its ability to bind with EA remains unchanged (unpublished results, personal communication with B. Strehlitz). The other sequences, EA1, EA1D, EA2, EA2D, EA2a, and EA2aD, are shortened derivatives that contain the core of G-rich regions from which G-quadruplex motifs can be formed. PAGE-purified DNA was dissolved in doubly distilled water prior to use. Single-strand concentrations were determined by measuring absorbance at 260 nm and 95 °C using molar extinction coefficients. The DNA concentration was determined using UV measurements taken on a Varian Cary (Amedis) 100 UV−visible spectrophotometer. A quartz cuvette with optical path lengths of 10 mm was used, and the temperature of the cuvette holder was controlled using an external circulating water bath. An aliquot of DNA from the stock solution was diluted in a buffer containing either 50 mM sodium or potassium chloride. The DNA sample was heated to 95 °C for 5 min and slowly cooled to 20 °C over the course of 1 h. Spectral measurements were performed after incubation for

dx.doi.org/10.1021/bi500773c | Biochemistry 2014, 53, 7013−7027

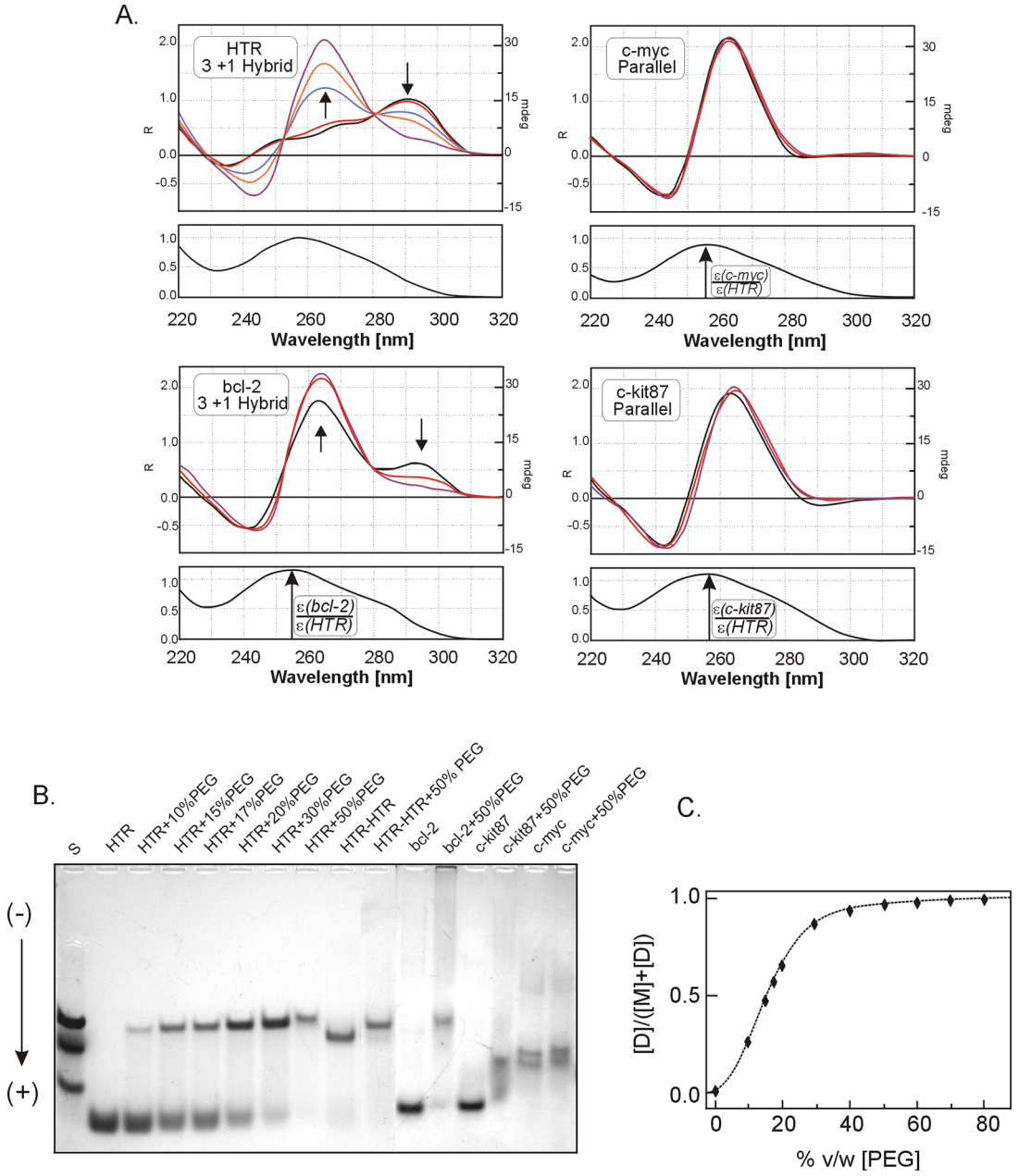

Figure 1. (A) CD spectra of HTR, bcl-2, c-myc, and c-kit87 oligomers in modified 25 mM Britton-Robinson buffer (pH 7.0) in the presence of 50 mM KCl (black lines). The samples of DNA contain 15% (v/w) PEG 200 (red lines), 30% (v/w) PEG 200 (blue line), 40% (v/w) PEG 200 (orange line), and 50% (v/w) PEG 200 (magenta). The increase and decrease in the magnitude of CD signals at antiparallel (3+1) hybrid G-quadruplexes at 265 and 295 nm, respectively, with increasing concentrations of PEG 200 are marked by black arrows. The corresponding UV spectra are shown under each panel with CD spectra. The concentration of DNA oligomer was adjusted individually for each DNA oligomer as described in Materials and Methods. (B) Electrophoretic record of the same DNA samples determined in the same type of buffer as the CD and UV measurements. Samples containing PEG 200 were heated to 95 °C for 5 min, slowly cooled, and then loaded into the electrophoretic wells. The S-line represents the mobility of the mixture of oligonucleotides: $d(AC)_9$, $d(AC)_{12}$, and $d(AC)_{18}$. (C) Dependence of HTR dimerization on PEG 200 concentration.

an additional 30 min at 20 °C, although in some electrophoretic experiments the cooling process was reduced to 30 min to prevent the formation of more complex multimolecular structures that require a longer time for their assembly. A modified Britton-Robinson buffer was used in all spectral and electrophoretic experiments. TRIS was used instead of KOH (NaOH) in this buffer: 25 mM phosphoric acid, 25 mM boric acid, and 25 mM acetic acid. The pH of the buffer was adjusted by titration of TRIS to a final value of 7.0. The main advantage of this buffer is that it allows the concentration of potassium ions to be modified without any change in pH; the buffer is also advisible for the electrophoresis.[18,21]

The concentration of DNA oligomers was determined on the basis of the Lambert−Beer law; the absorbance of the DNA sample depends on the concentration of DNA and the length of solution through which the light has passed. If $A = \varepsilon_\lambda cL$, then $c = A/\varepsilon_\lambda L$. For linear DNA molecules, the total extinction coefficient $\varepsilon_\lambda(\sum)$ consisted of the sum of $\varepsilon_\lambda(Q)$ and $\varepsilon_\lambda(P)$, where Q and P represent the numbers of nucleotides forming G-quadruplexes and the number of protruding nucleotides that are not associated on the G-quadruplex structure, respectively.

dx.doi.org/10.1021/bi500773c | *Biochemistry* 2014, 53, 7013−7027

The molar extinction coefficient depends on the wavelength λ. The $\varepsilon_\lambda(Q)$ of the linear oligonucleotide is slightly different from that of the folded G-quadruplexes, a finding that can be explained by the absorption TDS. The ε_{260} of folded oligomers is slightly smaller than that of unfolded complexes, so the molar concentration of DNA in cases where only unfolded DNA oligomers occur in solution was determined using UV−vis spectroscopy at a temperature that is greater than the melting temperature of the G-quadruplex. Thus, the precise concentration of any DNA oligomer can be obtained only in the absence of monovalent ions or more preferably at higher temperatures at which G-quadruplexes occur in an unfolded form.

Circular Dichroism Study. CD spectra were recorded on a Jasco (Easton, MD) J-810 spectropolarimeter equipped with a PTC-423L temperature controller using a quartz cell with a 1 mm optical path length in a reaction volume of 150 μL. All other parameters and conditions were the same as those that have been described previously.[21,22] The concentration of DNA oligomers was adjusted to 4.5 μM.

The parameter R was calculated on the basis of the CD spectra results. R is defined as

$$R = [\mathrm{CD}(295) + \mathrm{CD}(265)]/\mathrm{CD}_{\mathrm{HTR}}$$

where $\mathrm{CD}(\lambda)$ is the intensity of the CD signal at wavelength λ and $\mathrm{CD}_{\mathrm{HTR}}$ is the CD intensity of the standard HTR sequence at 295 nm.

CD Melting Curves and Thermal Difference Spectra. CD melting profiles were collected at 295 and 265 nm. The thermal stability of the quadruplex-forming sequences was also measured by recording UV absorbance at 295 nm as a function of temperature using a method similar to that previously published.[14] The temperature ranged from 10 to 100 °C, and the heating rate was 0.25 °C/min. Thermal difference spectra (TDS) were obtained through the subtraction of UV spectra measured at 95 and 10 °C, respectively.[23] The melting temperature (T_m) was estimated from the peak value of the first derivative of the fitted curve.

Electrophoresis. Native polyacrylamide gel electrophoresis (PAGE) was performed in a standard temperature-controlled vertical electrophoretic apparatus at a gel concentration of 15% [19:1 acrylamide:bis-acrylamide ratio (Applichem, Darmstadt, Germany)]. Approximately 1.5 μg of DNA was loaded onto each well of a 14 cm × 16 cm × 0.1 cm gel. Electrophoreses were performed at 8 and 40 °C for 4 h at 125 V (~8 V cm^{-1}). DNA bands were visualized with Stains-all immediately after electrophoresis, and the electrophoretic results were photographed on a white pad with a standard Nikon D3100 digital camera.

RESULTS AND DISCUSSION

Quantification of the CD Signal. Circular dichroism (CD) spectroscopy can be used to determine G-quadruplex structure formation within G-rich sequences, but the method can also be combined with other techniques to identify specific types of quadruplex folds.[24,25] However, it should be pointed out that this method of interpreting CD data in terms of G-quadruplex topology is still a matter of controversy because the orientation of the DNA strand is not the main determining factor where these positive and/or negative peaks are observed; the stacking arrangements of guanine residues also play a significant role.[26−28]

Usually, the parallel and antiparallel topologies of G-quadruplexes can be identified by determining the position of the positive peak in CD spectra in the range of 230−320 nm. Parallel G-quadruplex structures exhibit a clear positive band at ~265 nm and a negative peak at ~240 nm, while antiparallel G-quadruplexes exhibit a positive CD signal at ~295 nm and a negative signal at ~265 nm. However, the so-called (3+1) conformer, in which three strands are in the same alignment but another strand is oriented in the opposite direction, exhibits a positive shoulder at 265−270 nm.[29] These spectral features are observed in G-quadruplexes due to specific guanine quartet stacking and the orientation of glycosidic bonds along the G-strands, features that are not found in unfolded DNA. It is also important to note that other structural forms may display a positive peak in the region of 265 nm, but this spectrum does not necessarily indicate the presence of a G-quadruplex.[21]

An important issue to consider is how large the maximal intensity of these characteristic peaks at 265 and 295 nm can be. One of the aims of this study is to quantify these parameters and also to ascertain whether this intensity is dependent on DNA topology. To establish this, a number of well-characterized G-quadruplexes, the structures of which have already been determined by NMR, were analyzed. The quartz cuvettes were found to contain the same amount of molecules, but the amount of nucleotides present was always different. These differences in oligonucleotide concentration were then compared with the intensity of peaks responsible for G-quadruplex formation in each case. Figure 1 shows the CD spectra and electrophoretic record of the following sequences: HTR, bcl-2, c-myc, and c-kit87. HTR and bcl-2 form the hybrid antiparallel G-quadruplexes in the presence of potassium, while c-myc and c-kit87 develop parallel forms.[14−17,30] The CD spectral results show positive signals at 265 and 295 nm. Both HTR and bcl-2 moved faster in the electrophoretic gel than c-kit87 and c-myc. The CD spectral results for c-myc and c-kit87 display a clear signal at 265 nm, a finding that corresponds to the formation of a parallel G-quadruplex. Interestingly, two bands of c-myc are visible; both of these bands are isoform structures, and their levels of mobility lie between those of HTR and HTR-HTR. Therefore, it was not possible to determine precisely whether these bands represent intermolecular or intramolecular structures on the basis of electrophoretic record and CD measurements. In addition, the mobility of these two bands at various concentrations of potassium in the range of 2.5−150 mM significantly was not affected (not shown). The CD intensity of c-myc showed only a small change even when PEG 200 was added and is approximately the same as that of HTR in the presence of 50% PEG 200. However, the influence of PEG 200 on the mobility of c-kit87 is far more evident. The electrophoretic band becomes smeared, and the most intense band displayed a level of mobility similar to that of the faster band of c-myc. There is no significant effect on the CD signal. It is possible to suggest that PEG 200 somehow influences the topology of the c-kit87 G-quadruplex.

The CD spectrum of HTR shows a main positive peak at 295 nm and a shoulder at 265−270 nm. HTR cannot be considered a "pure" antiparallel G-quadruplex, as a positive signal was recorded at 265 nm, a result that is in contrast to that of TBA. A pure antiparallel G-quadruplex should have a negative signal at 265 nm. However, the G-quadruplexes that have been studied in most detail are known to consist of three G-quartets, while TBA contains only two; this important difference renders

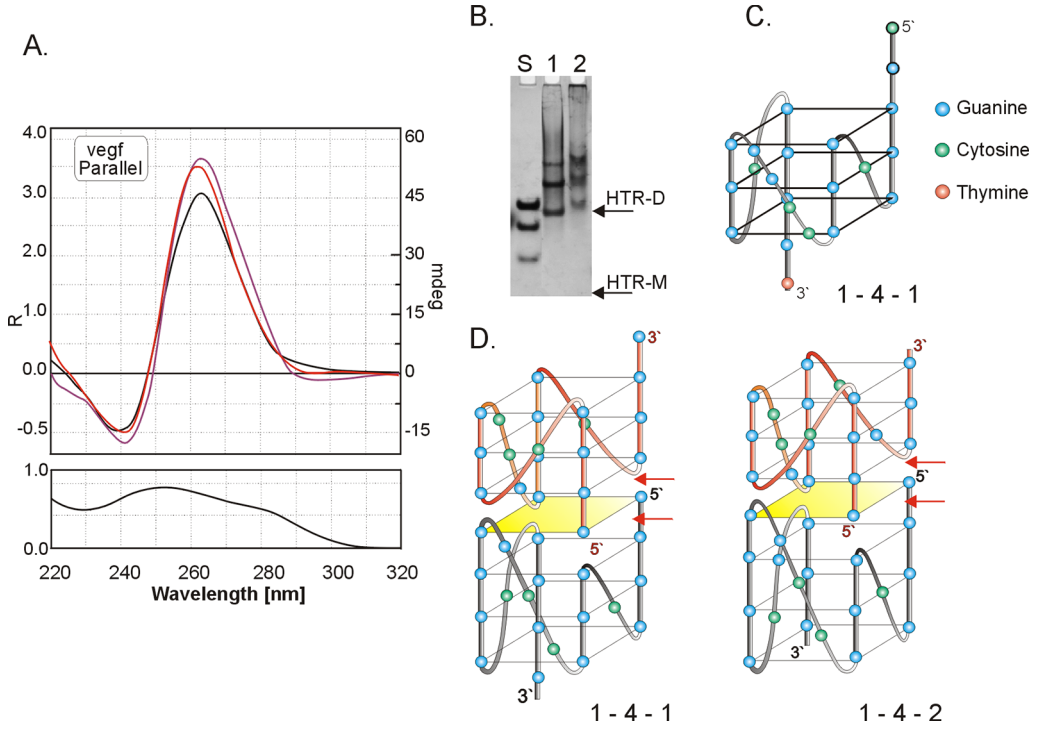

Figure 2. (A) Electronic CD spectra of vegf oligomers in modified 25 mM Britton-Robinson buffer in the presence of 50 mM KCl (black) and after addition of 15% (v/w) PEG 200 (red) and 50% (v/w) PEG 200 (magenta). (B) Electrophoretic record of vegf: line 1, no PEG 200; line 2, 50% PEG 200. The S-line represents the mobility of the same standard that was used in Figures 1B and 4. The mobilities of HTR monomer and dimer are marked by arrows. (C) NMR structure of vegf that has been described previously.[12] The number of oligonucleotides forming three loops in the G-quadruplex is 1−4−1. (D) Two proposed models of the dimeric structure of the vegf G-quadruplex differing in their loops.

TBA an appropriate standard for our purposes. Other sequences with the ability to form three-stack G-quartet quadruplexes were evaluated in the presence of potassium ions, but we were unable to find a single DNA oligomer that formed a G-quadruplex without a positive CD shoulder at ~265 nm; in all cases, a shoulder of some kind was observed. However, most of the antiparallel G-quadruplexes exhibiting positive shoulders also formed antiparallel structures without this shoulder when the potassium ions were replaced with sodium. Previous work has shown that the binding mode of these two ions is not the same; sodium is bound in the central cavity of each G-quartet, and potassium is placed between two G-quartets. This would mean that the core of G-quadruplexes differs depending on the presence of either potassium or sodium, thereby indicating that the intensity of the CD signal would be different at 265 and/or 295 nm.

PEG 200 is a valuable dehydrating agent that has an influence on quadruplex topology in the presence of potassium.[18,31,32] Interestingly, the stabilizing quality of PEG 200 does not seem to have any effect on three-quartet antiparallel G-quadruplexes; the presence of isodichroic points at 253 and 280 nm suggests that these structures are converted to parallel conformers in the presence of both potassium and PEG 200 (Figure 1). However, the concomitant effect is a multimerization of HTR G-quadruplex (panels B and C), the relative CD intensities of which are directly visible in the CD spectra in Figure 1. DNA oligomers consisting of eight G-runs, HTR-HTR, were also loaded into the electrophoretic well to determine the molecular size of the slower band of HTR that was formed in the presence of PEG 200. The HTR-HTR oligomer has been shown to possess the ability to form two quadruplexes arranged in tandem.[33] The mobility of HTR-HTR corresponds with this slower band of HTR, so it is therefore possible to suggest that this band represents the dimeric form of HTR. However, this then raises the question of whether an intramolecular and antiparallel G-quadruplex is formed without the multimerization induced by PEG 200 during the conversion to parallel forms in the presence of potassium. Our analysis did not find any G-quadruplex that fulfilled these criteria, and therefore, HTR was chosen for use as a standard. The CD signal of HTR in the presence of 50% PEG 200 is approximately 2.25-fold higher at 265 nm than the signal in the absence of PEG 200 at 295 nm. This suggests that antiparallel structures are converted to completely parallel forms at higher concentrations of PEG 200 (Figure 1C). Similar results were also obtained for oligomer bcl-2 in the presence of PEG 200, but the shift in the bcl-2 CD signal is much smaller than that of HTR. However, the intensity of CD signals of parallel c-myc and c-kit87 G-quadruplexes in the presence of 50% PEG 200 did not show any significant change, and no structural conversion was observed. The multimeric analogue of G-quadruplexes that occur in an antiparallel monomeric intramolecular form is usually parallel, although this effect is predominantly observed in buffers containing potassium. It is also important to note that some G-quadruplexes are not converted to parallel structures in the presence of crowding or dehydrating agents; e.g., TBA is anchored in a monomeric antiparallel form (not shown).

The intensity of the CD signal at 265 nm of three-quartet G-quadruplexes in the presence of potassium is approximately 2 times higher than the value that can be reached at 295 nm. This implies that an intramolecular parallel G-quadruplex would show a CD signal that is twice as intense as that of an antiparallel form. When the maximal intensity at 295 is not saturated, a positive signal is observed at 265 nm. A decrease in

dx.doi.org/10.1021/bi500773c | *Biochemistry* 2014, 53, 7013−7027

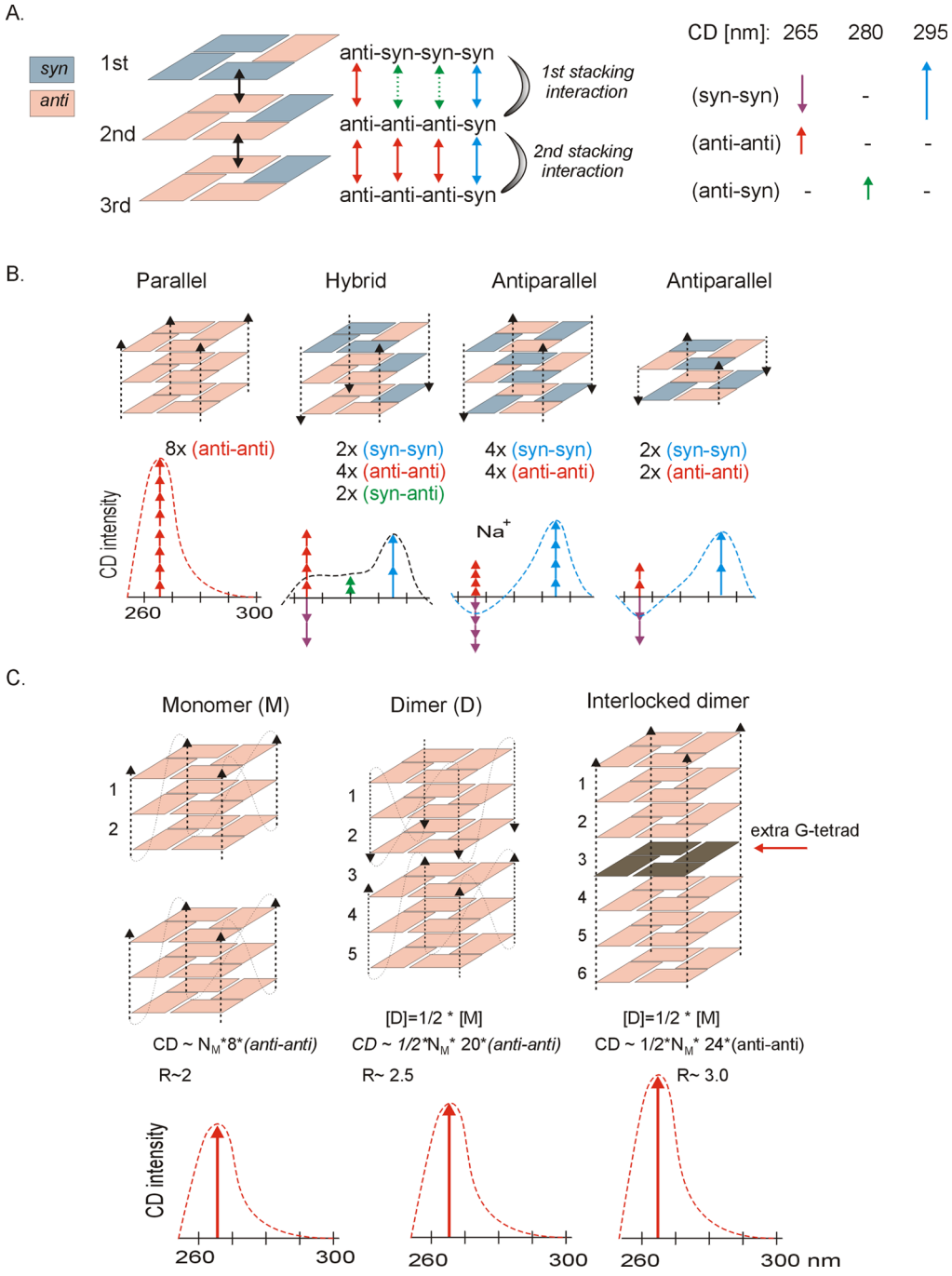

Figure 3. Schematic illustration of the model used in this study. (A) G-Quartet consisting of four guanines. The conformations of *syn*- and *anti*-guanines in a G-quartet are shown by different colors. The virtual blue, magenta, and red vectors represent a partial contribution of G-quartet stacking interaction and an image of the CD signal at 265 and 295 nm. The red vector of the (*anti*−*anti*) interaction contributes to the positive CD signal at 265 nm, while the blue and magenta vectors of the (*syn*−*syn*) interaction contribute to the positive and negative signals at 295 and 265 nm, respectively. The green vector represents a (*syn*−*anti*) interaction. (B) The hybrid HTR quadruplex consists of seven *anti*-guanines and five *syn*-guanines; the result is a positive signal at 295 nm consisting of two (*syn*−*syn*) interactions and a positive shoulder at 265 nm consisting of four (*anti*−*anti*) and two (*syn*−*anti*) partial interactions. A three-quartet parallel G-quadruplex consisting of 12 *anti*-guanines forms eight (*anti*−*anti*) partial interactions; the CD signal consists of eight red vectors at 265 nm only. (C) Examples of two parallel monomers, a stacked dimer and an interlocked dimer with an extra quartet depicted at the bottom margin. An interlocked dimer that consists of one extra G-quartet shows a CD signal at 265 nm ~50% stronger than that of the monomer.

the CD signal at 295 nm induces 2−2.3-fold increases in the CD signal at 265 nm. However, the vegf sequence demonstrates a CD signal that is 3 times higher at 265 nm in the absence of PEG 200 and >3.5-fold higher in the presence of PEG 200 (Table 1 and Figure 2). This sequence folds into a three-quartet G-quadruplex in the presence of potassium (Figure 2C).[12] One possible explanation for the unusual properties of this DNA oligomer is based on the results of electrophoretic separation under corresponding conditions. The electrophoretic record shows the presence of both the dimer and highly ordered structures regardless of whether PEG 200 was present.

dx.doi.org/10.1021/bi500773c | *Biochemistry* 2014, 53, 7013−7027

Table 2. Parameters Obtained in the Experiments[a]

	CD signal in Na^+		CD signal in K^+		melting temperature at 50 mM (°C)		molar dichroism ratio			
abbreviation	265 nm	295 nm	265 nm	295 nm	NaCl	KCl	R_{Na}	order	R_K	order
HTR	−	+	+	+	*52.8*	*63.2*	1.0	M	1.0	M
oncogenic sequences										
bcl-2	+	+	+	+	*55.2*	*74.5*	1.1	M	1.5	M
c-myc	+	−	+	−	45.7	86.5	2.1	M, D$^{\#}$	2.3	M/D?
c-kit87	+	+	+	−	26.8	57.8	1.9	M, H	2.0	M
vegf	+	+	+	−	*47.5, 72.1*	81.6	1.1	M, H$^{\#}$	3.0	D, H
aptameric sequences										
EA1−42	+	−	+	−	31.5	58.5	1.2	M	2.8	M, D, H
EA1	+	−	+	−	33.0	70.5	2.6	D	2.5	D
EA1D	+	−	+	−	50.0	90.0	3.4	D	2.7	D
EA2	+	−	+	−	31.0	67.0	1.7	M, D$^{\#}$	2.3	M
EA2D	+	−	+	−	55.0	89.5	2.9	M, D_1, D_2	2.5	M, D$^{\#}$
EA2a	+	−	+	−	34.0	72.5	2.7	D	2.2	D_1, D_2
EA2aD	+	−	+	−	53.0	93.0	3.1	D	2.7	D
HCV	+	−	+	−	44.0	72.5	3.2	D_1, D_2, H	2.9	D, H$^{\#}$
Hema	−	+	+	−	ND	70.5	0.5	D	2.7	D
HIV-93del	+	−	+	−	61.5	>95	2.9	D, H_1, H_2	2.5	D, H_2
Insu	+	−	+	−	44.5, *26.5*	52.0	1.5	M$^{\#}$, D, H	2.4	M$^{\#}$, D, H
IonK	−	+	−	+	46.0	59.0	0.9	M	1.0	M
Scle	+	−	+	−	61.2	81.5	3.1	D, H	2.8	D
Stat	+	−	+	−	54.5	93.5	3.1	D	2.7	D
TBA	−	+	−	+	13.5	47.0	1.0	M	1.0	M
TNF	−	−	−	−	ND	ND	0.3	M	0.3	M
apVEGF-D	+	+	−	+	46.0	49.5, *52.0*	0.9	M	1.3	M$^{\#}$, D, H
apVEGF	−	+	+	+	45.0	48.0, *37.5*	0.5	D	1.5	M, D, H

[a]The deviation at the determination of melting temperature is ±1.5 °C. The errors in determining factors R_{Na} and R_K are 15%. ND means not determined. The lower index value represents the wavelength at which the value was determined. M is monomer; D is dimer, and H is highly ordered structures at 25 °C. The number signs indicate very small populations. The melting curves obtained at 295 nm are written in italics. The concentration of DNA oligomers was ∼4.5 μM.

Model Predicting Multimerization. The intensity of the CD signal is clearly dependent on the amount of stacked quartets, but does this also mean that multimeric G-quadruplexes consist of more stacked quartets? A hypothesis regarding the multimerization process of parallel G-quadruplexes is depicted schematically in Figure 3. The total number of G-quartet stacking interactions for N molecules folded into G-quadruplexes consisting of three G-quartets is $2N$. When all molecules form m-mer complexes consisting of three quartets, the total number of these interactions is $2N + (m - 1)N/m$; m is 2 for dimer, 3 for trimer, etc. The relative increase in the number of G-quartets is $(m - 1)/2m$ during m-merization; for example, dimerization causes a 25% increase in the number of stacked interactions, tetramerization 37.5%, octamerization 43.7%, etc. (Figure S1 of the Supporting Information). Each G-quartet consists of four guanines that occur in either a *syn* or an *anti* conformation. In our model, we suggest that two neighboring G-quartets interact with each other and that this interaction is the main contributor to the CD signal. The basic principle of the model is illustrated in Figure 3A. We suggest that the *syn*- and *anti*-guanines in one layer preferentially interact with the *syn*- and *anti*-guanines in the neighboring layer, respectively. These interactions are (*syn*−*syn*) and (*anti*−*anti*). Once these homogeneous couples have formed, the remaining unpaired bases form a mixed (*syn*−*anti*) interaction. However, this form of pairing can only be considered as an additional contributor of stacking interactions in G-quadruplexes. The virtual vectors of this interaction are shown as the partial images of the CD spectra. The red vector of the (*anti*−*anti*) interaction contributes to the positive CD signal at 265 nm, while the blue and magenta vectors of the (*syn*−*syn*) interaction contribute to the positive and negative signals at 295 and 265 nm, respectively. In the presence of potassium, we suggest that the red vector is half the size of the blue vector and that the magenta vector is approximately one and one-half times the size of the red vector, although these proportions may not be valid in a sodium buffer. The (*syn*−*anti*) form of interaction is represented by the green vector that contributes to a positive signal at ∼280 nm. The size of the green vector is a half or less than half of that of the red vector. Figure 3B shows the cases of four different conformations of G-quadruplex: parallel, hybrid, antiparallel, and two-layer antiparallel structures. The dimeric and interlocked G-quadruplexes with one extra quartet that consist of only *anti*-guanines are shown in panel C.

Generally, a mixed population differing in the number of subunits can coexist in solution, e.g., N_1 monomers, N_2 dimers, N_3 trimers, N_4 tetramers, etc.

$$N = N_1 + N_2 + N_3 + \ldots + N_j$$

However, the conformation of the guanines in the G-quartet significantly influences the intensity of the peak in the CD spectrum. Analogically, this model can also be extrapolated for G-quadruplexes consisting of different numbers of quartets, for example, two, four, five, etc.

dx.doi.org/10.1021/bi500773c | *Biochemistry* 2014, 53, 7013−7027

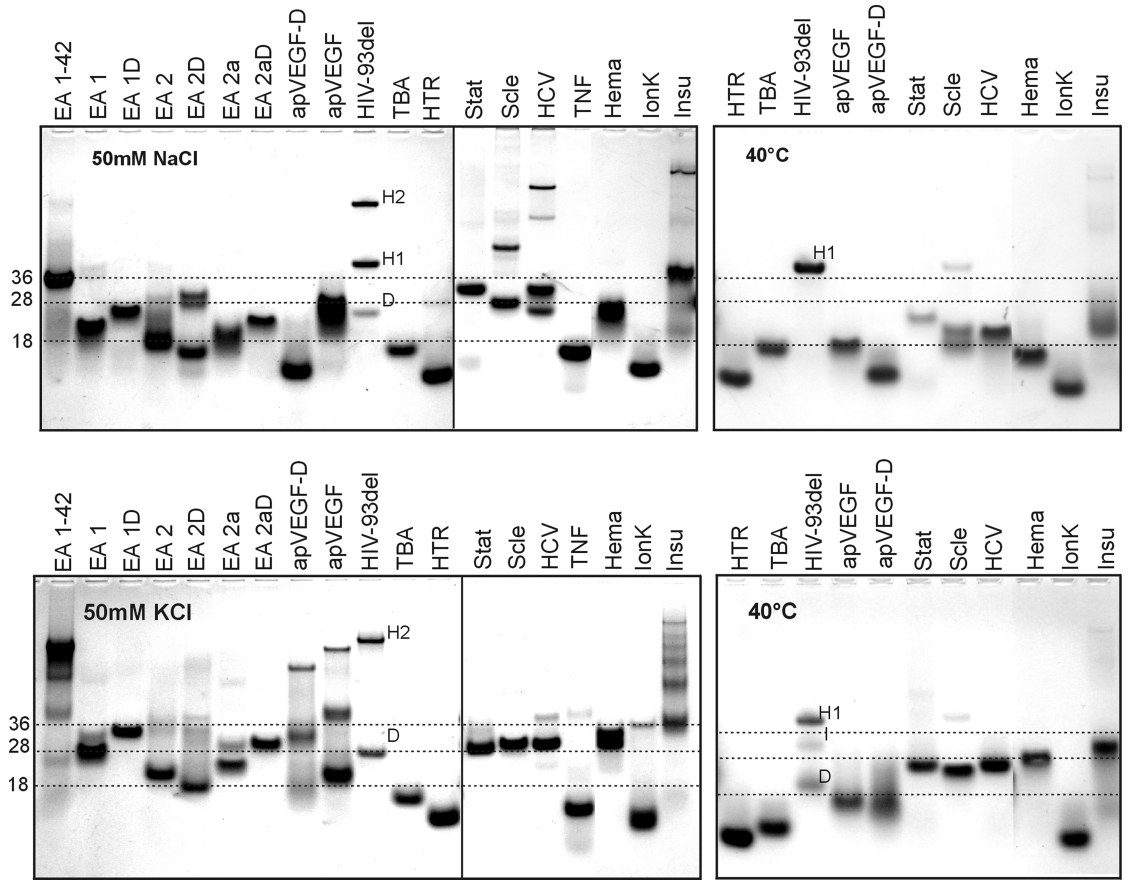

Figure 4. DNA aptamers resolved by gel electrophoresis and visualized with Stains-all staining. Molecular standards, a mixture of $d(AC)_9$, $d(AC)_{12}$, and $d(AC)_{18}$ (dashed lines), and HTR were used. Electrophoretic separation was performed in a 15% polyacrylamide gel at 8 °C (left) and 40 °C (right) in 25 mM Britton-Robinson buffer (pH 7.0) and 50 mM NaCl (up) and 50 mM KCl (down). Prior to being used, the DNA samples were heated in the same buffer for 5 min at 95 °C and slowly cooled to room temperature over the course of 1 h; the samples were incubated at 20 °C for an additional 30 min. The DNA samples in the right gels were cooled within 15 min, and no incubation was performed prior to use. The positions of the dimer and highly ordered forms are marked by D, and H, respectively.

An increase in the number of stacking interactions of G-quartets in vegf multimers could be responsible for the significant increases in CD intensity at 265 nm. The CD signal of vegf is 1.5-fold stronger than that of HTR at 265 nm in the presence of 50% PEG 200 or 3-fold stronger than that of HTR at 295 nm in the absence of PEG 200. CD and electrophoretic results show that the vegf oligomer forms dimer, tetramer, and also highly ordered structure, and these structural variants make a substantial contribution to the increases in the CD signal. Electrophoretic results show that the addition of PEG 200 results in a slight increase in the population of multimers in vegf; an increase in the strength of the CD signal is also observed. On the basis of these results, we suggest that the dimer consists of two parallel G-quadruplex subunits with loops 1−4−1, resulting in an interlocked structure with one more G-quartet (Figure 2D). The structure of vegf as determined by other authors contains one additional C at the 5′ terminus.[12] This would suggest that such a molecule has performed two additional stacking interactions instead of only one (indicated by red arrows in Figure 2). It is also possible to suggest that an alternative folding process[1−4] that does not form any obstacle during tetramerization of two dimers has taken place; this hypothesized assembly of vegf G-quadruplexes would explain the strong dichroic signal at 265 nm. However, it is important to stress that this hypothesis needs to be verified by further research.

The same effect should also occur in the process of dimerization for c-myc and c-kit87; however, the error margin of the ratio *R* for these complexes is approximately 15%, and thus, the effect is less significant than that observed for oligomer vegf. In addition, c-kit87 in 50% PEG 200 does not show the same tendency to dimerize that is seen in other oligomeric DNAs; during electrophoresis, a smear between the monomeric and dimeric forms was observed under these conditions.

On the basis of this set of observations, it is possible to conclude that the CD intensity of any G-rich oligomer that can form a three-quartet intramolecular G-quadruplex reaches its maximum of CD spectra at 265 and 295 nm; this does not deviate significantly from the values obtained for HTR at 295 nm or c-myc at 265 nm in the presence of 50 mM KCl. Although the CD intensity is higher in comparison with the intensities of these two standards, it is very likely that higher multimeric forms are formed in solution.

The results discussed above indicate that it is possible to develop a model for predicting multimerization in G-quadruplexes based on the comparison of CD spectra of specific G-quadruplexes with those of a standard G-quadruplex. As was noted above, HTR is used as the standard for three-quartet G-quadruplexes. The model that we propose in this study is based on the parameter *R*.

dx.doi.org/10.1021/bi500773c | *Biochemistry* 2014, 53, 7013−7027

We propose the following rules based on the value of this R parameter.

(1) If three-layer intramolecular G-quadruplexes form additional stacking interactions between different G-quadruplex molecules, then R should be >1 for antiparallel G-quadruplexes and range from 2.0 to 2.5 for parallel G-quadruplexes.

(2) If R is significantly less than 1, then either very few molecules form a three-layer G-quadruplex or G-quadruplexes with fewer than three G-quartets are formed. Other secondary or unfolded structures can also be present under the given conditions.

(3) If R is greater than 2.5, then at least one intermolecular or interlocked conformer (dimer, trimer, tetramer, etc.) is very likely. These highly ordered G-quadruplexes consist of at least four quartets, e.g., vegf sequence.

The relative intensities of the CD signals, parameters R_K and R_{Na}, in Table 2 depict the comparison with the standard HTR in the presence of 50 mM NaCl and KCl, respectively.

The latter parameters are useful in estimating the relative formation of stacked G-quartets in unknown sequences in comparison with those formed in HTR. It is presumed that the contribution of G-quartet stacking interactions to the CD signal does not depend significantly on the loops of G-quadruplexes, but only on the orientation of strands. While we remain aware of the weakness of this presumption in our comparison of G-quadruplexes consisting of different numbers of G-quartets, e.g., two in TBA and three in HTR, we still maintain that these parameters are valuable in predicting the existence of additional stacking between G-quadruplexes (Figure 3). However, the results of electrophoretic separation can offer more evidence than the results of spectral measurements with regard to the presence of multimeric isoforms in which more stacking interactions occur (Figure 4). While these analyses are useful and pertinent, it is nonetheless necessary to compare these estimates with results obtained using other methods such as electrophoresis, mass spectrometry, and NMR. A similar comparison of the maxima of molar circular dichroism and electrophoretic mobility for sequences such as $d(G_3T)_3G_3$, $d(G_3T_2)_3G_3$, $d(G_3T_2)_3G_3$, and $d(G_4T_2)_3G_4$ with those of HTR has been performed previously[18] (see also Table S1 of the Supporting Information). Our model allows an estimate to be made of the level of stacking in G-quadruplexes with additional G-quadruplex structures, but it is not able to calculate exactly how many G-quartets contain some type of G-quadruplex structure. For example, oligonucleotide $dG_3T_2AG_3$ forms a bimolecular G-quadruplex and R_K is ~0.5. This suggests that the concentration required to achieve the same amount of G-quartets as in HTR would have to be twice as high. It is also possible to apply our model to shorter sequences such as d(GGGTTAGGG) and d(TTGGGGGGGTT) (Table S1 of the Supporting Information).

CD Spectroscopy of DNA Aptamers. The information obtained in these initial experiments was then applied to other DNA aptameric sequences in an effort to prove that stacked G-quartets are the main contributor to the CD signal at 265 and 295 nm. It was also anticipated that the intensity of the molar CD signal could be proven to be dependent on the total number of stacked G-quartet interactions and the conformation of guanines.

Figure 5 shows the CD spectra and TDS of aptameric DNA oligonucleotides in the buffers containing 50 mM KCl (black lines) and 50 mM NaCl (blue lines), respectively. The profile of the *IonK* spectrum fits well with the spectrum of HTR that

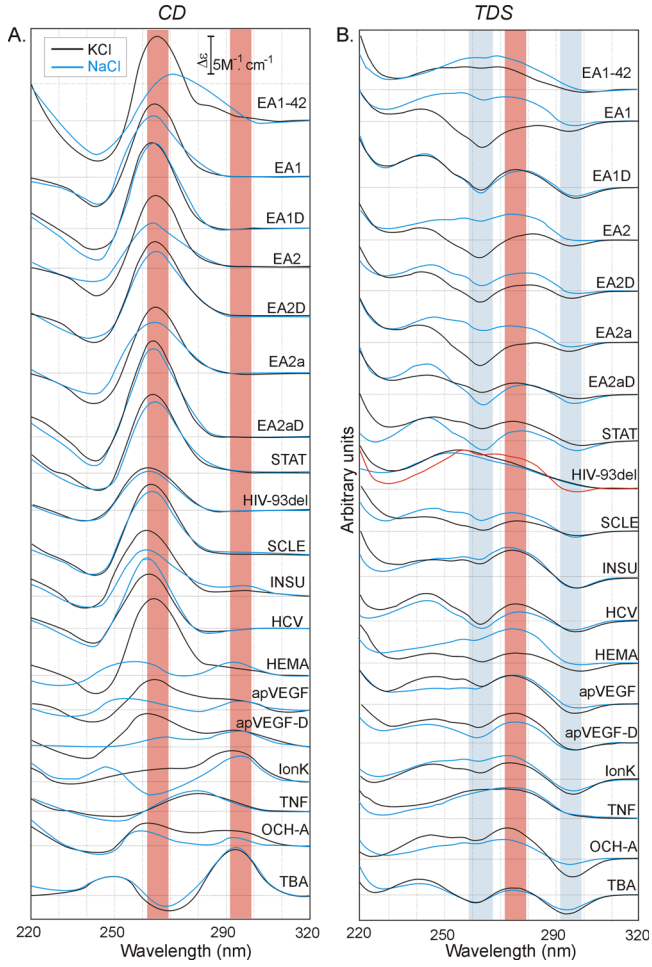

Figure 5. (A) Electronic CD spectra of G-rich oligomers in modified 25 mM Britton-Robinson buffer (pH 7.0) in the presence of 50 mM KCl (black) and 50 mM NaCl (blue). (B) Corresponding TDS obtained. The spectrum obtained in the absence of ions is represented by a red line. The highlighted red and blue bands correspond to positive and negative regions, respectively, which are typical for G-quadruplexes.

shares the (3+1) arrangement of strand orientation in the presence of potassium.[29] The same sequence forms antiparallel G-quadruplexes in the presence of sodium and is also a perfect fit with the CD spectrum of HTR. As mentioned above, TBA is the only oligomer that was found to form antiparallel conformers in the presence of both sodium and potassium ions; the spectrum of TBA displays only one positive signal at 295 nm without any shoulder and one negative signal at ~265 nm in the range of 250−320 nm. With the exception of TNF, all other oligomers exhibit more dominant positive peaks at ~265 in the presence of both types of ions, with three of the aptamers, Hema, apVEGF, and apVEGF-D, also showing peaks at 295 nm. The CD profile of TNF fulfills none of the criteria for G-quadruplex formation; only a wide positive peak at 280 nm is seen in the presence of both ions.

TDS of Aptamers. Analysis using thermal difference spectroscopy is another indirect approach that can offer valuable information about the formation of G-quadruplexes from the DNA sequence. Figure 5 shows the thermal difference spectroscopy results of aptameric DNA oligonucleotides in buffers containing 50 mM KCl (black lines) and 50 mM NaCl (blue lines). The regions displaying important G-quadruplex

dx.doi.org/10.1021/bi500773c | *Biochemistry* 2014, 53, 7013−7027

signatures are highlighted by red (positive) and blue (negative) strips with the center at ~295, ~265, and ~270 nm. These results indicate the existence of G-quadruplexes for all of the studied oligomers under the given conditions with the exception of EA1−42, HIV93del, and TNF. However, the EA1−42 oligomer shows an inconspicuous but detectable signal in all three wavelength regions in the presence of 50 mM potassium. Previous studies have shown that the HIV93del aptamer forms interlocked dimeric G-quadruplexes that are extremely stable,[34] most likely a result of the five quartets in their structure, and therefore, the TDS for this oligomer are not as characteristic as those of the other, less stable quadruplexes at significant regions. Therefore, thermal difference spectroscopy was also performed at different concentrations of ions in the buffer, ranging from 0.5 to 5 mM. As shown by the red line in Figure 5, the results indicate that the G-quadruplex is formed in buffer containing only a residual amount of salts. Because of the extreme stability of the HIV93del aptamer, the UV spectrum recorded at 95 °C does not represent an already totally unfolded structure; in this case, thermal difference spectroscopy cannot represent clearly the spectral difference between folded and unfolded structures.

Our results show that TDS results can be ambiguous and that care should be taken in evaluating these findings. Any evaluation is highly dependent on the sequence; the sequence could either form an extremely stable G-quadruplex or unfold into this structure, and the main signatures would be undetected in either case.

The results obtained through two different experimental methods appear to suggest that TNF cannot be considered a G-quadruplex-forming aptamer as recent studies have suggested.[35] The EA1−42 aptamer also exhibits the signatures required for the existence of G-quadruplexes in the presence of potassium, although it is possible that this structure is already partially unfolded at 20 °C in the presence of sodium; the melting temperature is 31 °C, and therefore, a negative peak at 295 nm was not clearly detected (Table 2 and Figure 6).

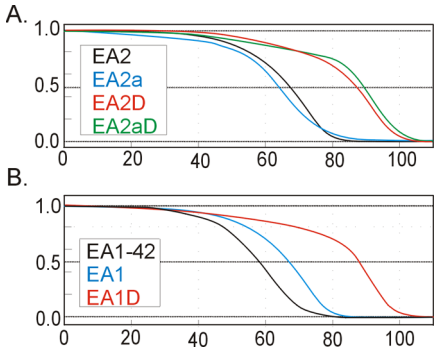

Figure 6. CD melting curves of EA aptamers collected at 265 nm in the presence of 50 mM potassium. Each melting curve represents original data that are shown in the interval between 0 and 1.

Thermal Stability and Molecularity of Aptamers. The melting temperature is another valuable thermodynamic parameter that can be used in the study of G-quadruplex aptamers. CD spectroscopy was used to obtain melting curves collected at 265 and/or 295 nm for all of the studied sequences; the results are summarized in Table 2 and Figure 6. As with all quadruplexes that have been studied to date, the aptameric molecules analyzed in this study were found to be more stable in the presence of potassium than in sodium. Polyacrylamide gel electrophoresis is a supplementary technique that can be used to determine the coexistence of various structural variants of aptamers under given conditions. Accordingly, electrophoretic separations were performed in the presence of sodium or potassium at two different temperatures, 8 and 40 °C (Figure 4), in an effort to demonstrate that some conformers convert to isomers with increased stability at higher temperatures.

The melting temperatures obtained from the set of oligomers derived from the ethanolamine aptamers (EA) proved to be of particular interest. The original aptamer EA1−42 shows low levels of stability and possesses a longer flanking sequence in place of a G-quadruplex-forming sequence. In the presence of sodium ions, this aptamer does not form a stable G-quadruplex structure and has a melting temperature of 31 °C. However, its melting temperature in the presence of 50 mM KCl is significantly higher (58.5 °C). Previous studies have found that overhanging nucleotides that are not directly associated in the quadruplex structure typically have a destabilizing effect on G-quadruplex stability.[36] The core of the EA1−42 sequence that forms G-quadruplex, EA1, is significantly more stable than the EA1−42 sequence itself, because of the destabilizing effect of the overhangs at both the 5′ and 3′ termini of the EA1−42 complex. Its melting temperatures in sodium and potassium buffers are 33 and 70.5 °C, respectively. The thermal stabilities of so-called bulged G-quadruplexes with "standard" structures have recently been compared using NMR and spectral measurements.[37] It was found that intramolecular G-quadruplexes with bulges can be formed but that their thermal stabilities are lower in comparison to those of G-quadruplexes without any bulges. The sequences EA1−42, EA1, EA2, and EA2a allow the formation of bulged G-quadruplexes. The melting temperatures of EA1D are 50 and 90 °C in sodium and potassium buffers, respectively. These melting temperatures are approximately 17 and 20.5 °C, respectively, higher than those of EA1. The same effect was observed for the EA2D−EA2 and EA2aD−EA2a couples (Figure 6). In addition, G-quadruplex(es) formed from shorter sequences of the EA2a−EA2 couple are more stable, because the 5′ overhanging sequence d(GCTG) contributes to the further destabilization of EA2 and EA2D (Table 2). However, this was not valid for the EA2aD−EA2D couple in the presence of sodium, a difference for which there are two possible explanations; either the protruding sequence d(GCTG) is somehow associated with the G-quadruplex structure, thereby resulting in a slight stabilization of EA2D, or alternatively, they form more topological forms that are visible in the electrophoretic pattern. The electrophoretic profiles of these two oligonucleotides are different despite the identical CD spectral results (Figures 4 and 5). EA2aD forms only one clear topological structure, but EA2D forms at least three different conformers with different melting temperatures. The melting temperature that was measured via CD spectroscopy is an average temperature of all three of these conformers occurring in solution. The electrophoretic mobilities of EA1, EA1D, EA2a, and EA2aD in the presence of sodium and potassium correspond to the dimeric form, and both ratios R_{Na} and R_K are >2 (Table 2 and Figure 4). A prevalent population of dimeric forms is also observed for EA2D in the presence of sodium (R_{Na} = 2.9). The electrophoretic pattern of EA2a in sodium is smeared in comparison with the pattern in potassium in which the presence of two conformers, at least one of which is an

dx.doi.org/10.1021/bi500773c | *Biochemistry* 2014, 53, 7013−7027

intermolecular dimer, can be seen. This fact can be explained as follows. The smearing could be attributed to the ability of the two conformers to convert between each other; in the presence of potassium, each of these states is more stable and results in the separation of the bands without any smearing. The mobility of the longest ethanolamine aptameric sequence, EA1−42, in a polyacrylamide gel is higher in the presence of sodium than that of the unfolded standard, and the position of this band corresponds to that of an intramolecular G-quadruplex. However, in the potassium buffer, at least four bands with increasing intensities depending on their molecularity are visible, a result that agrees with the ratio R_K. The mobility of the darkest band could indicate the presence of at least a dimeric structure.

The core sequence of EA1D and EA2D is the same as those of HIV aptamers T30695 and T40214.[38] Aptamer EA1 is very similar to HIV integrase inhibitor T30177, with the T being replaced by an A in the case of EA1.[39] However, this base exchange has no significant effect on the formation of the dimeric stacked conformer of EA1.

The bulges are frequently an important element in determining the binding affinity and recognition between the G-quadruplex moiety and the target molecule. However, it seems that the bulges in the EA1 and EA2 aptamers are not essential for ethanolamine recognition because the binding constants of similar sequences were not affected significantly.[40] The authors analyzed very similar aptameric sequences differing only in one protruding nucleotide.

The HIV-93del aptamer also shows high levels of stability; its melting temperature is >95 °C in the presence of 50 mM potassium. This thermal stability is a result of the five stacked G-quartets in which the central quartet is interlocked and also of the central adenine residue that contributes to this stacking interaction.[34] In addition to this interlocked dimeric form, the HIV-93del aptamer also folds into other high-molecular conformers that can be detected using electrophoretic separation (Figure 4). Very clear bands were observed in the presence of sodium and potassium ions, and their mobilities are significantly lower than those of the interlocked dimers that have been studied by other authors.[38,41,42] The molecular mass of the second and third slower conformers is between 2 and 4 times greater than the first band representing the dimeric conformer. The slowest band could be a result of either the dimerization of two interlocked structures or the association of four oligonucleotides with different topologies (Figure 6). R_{Na} and R_K factors above 2.5 indicate that highly complex structures can exist in solution, but the structure representing the slowest band requires a longer time scale for its assembly because of the slow kinetics of formation. The model of the tetrameric conformer shown in Figure 7 clearly shows high levels of stability; the existence of a band with slower mobility and slower kinetics of formation can be explained on the basis of the number of molecules required for such assembly. For example, the tetramer is stabilized by 11 G-quartets and also by the common interlocking G-quartet consisting of guanines (Gs) originating from each of the four DNA oligomers; two Gs are common for one dimer and another two for the opposite dimer. Both dimers are arranged in a head-to-head direction. This interlocking arrangement of the dimer is very similar to that described recently in the N-myc intron sequence.[43] An additional increase in the level of supramolecular assembly is hindered by the terminal A residues at the 3′ terminus of each DNA oligomer. These protruding adenines (As) cause a steric

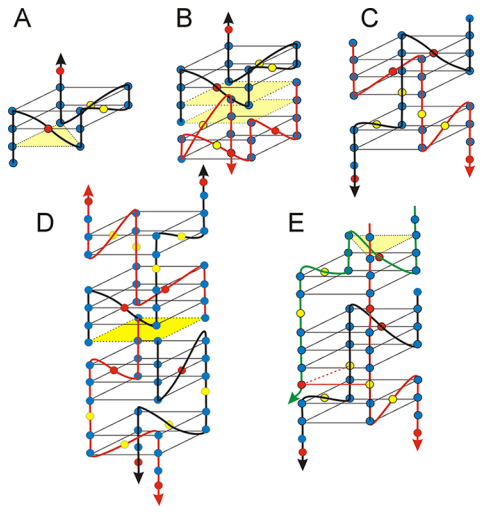

Figure 7. Schematic representation of G-quadruplex structure of the HIV-93del sequence. (A) Monomeric subunit that forms an interlocked dimer. (B) Structure of the interlocked dimer that was described in the presence of potassium by Phan et al.[36] (C) Proposed dimeric structure that can dimerize to an interlocked tetramer (D). (E) Proposed trimer structure that could form in the presence of sodium. The common G-quartet is colored yellow. The potential A-T bond is highlighted by red lines.

hindrance to the assembly of a head-to-tail arrangement; a similar G-wire limitation has been observed previously.[44] Further evidence confirming the slightly different structure of the HIV93del tetramer is provided by the color of the band of this molecule after the staining procedure. All electrophoretic bands are blue, but this band is purple (not visible in black and white representation). When the sample of DNA was incubated for a very short time and heated in the absence of potassium ions, the tetrameric band was not observed due to the fact that the conformer had not had enough time to assemble. A similar result was observed even after the addition of potassium to the cooled sample. However, when the electrophoresis was performed at 40 °C and the sample was prepared using a "slower procedure", the incubation and cooling periods were longer, and the tetrameric band was again visible (not shown). The tetramer always arises after incubation for several hours and is less dependent on the heating and cooling procedure, although the HIV93del aptamer in the presence of potassium forms other intermediate folds (I) when the cooling process is faster. The weaker intensity of the bands indicates that the population of the aptamers is lower. The trimeric conformer (H1) can also be observed in the electrophoretic record shown in Figure 4. This band is barely visible in the buffer containing potassium at 8 °C, but its population is clearly visible in the buffer containing sodium and also at lower concentrations of potassium (not shown). A possible fold of trimeric structure is also shown in Figure 7. The formation of this conformer requires three DNA strands, and additional condensation is not facilitated by cohesive heads or tails as was observed for the dimeric form. The interlocked dimer and tetramer may be more stable in comparison to the trimer, which could explain why this structure is less common in the presence of potassium, but the trimer can arise more easily in the sodium buffer than the tetramer. The mobility of G-quadruplexes increases linearly with temperature; therefore, the positions of the corresponding bands are slightly further from the electrophoretic starting point at 40 °C.[18] The melting curve profiles also suggest that more

dx.doi.org/10.1021/bi500773c | *Biochemistry* 2014, 53, 7013−7027

than one conformer exists in solution. When only one conformer melts, then the melting curve shows a sigmoidal shape that is characteristic of a two-state mechanism of unfolding, although this was not observed in the case of the HIV93del aptamer (not shown).

In the presence of sodium, the HCV (hepatidis C virus) oligomer forms four different conformers that could be clearly distinguished by electrophoretic separation. The average melting temperature is 44 °C, and the CD signal at 265 nm is 3.2 times stronger than that of HTR at the same molar concentration of DNA strands, which would indicate the presence of intermolecular conformers together with intramolecular forms. However, in the potassium buffer, only two conformers were detected by electrophoresis, and their average melting temperature is 72.5 °C. On the basis of these results, it is possible to suggest that the dimer is the most abundant conformer. This sequence has the ability to form two types of dimers with differing mobilities, but it can also form the bulged structure in which the bulge could emerge in the second G-run. The conformational variability of HCV is higher in the presence of sodium. Although the higher molecular conformers are formed more slowly, there is some analogy with the HIV-93del aptamer.

The Hema aptamer (hematoporphyrin IX) forms an antiparallel dimer in the presence of sodium, but the weaker CD signals at 295 and 265 nm (R_{Na} = 0.5) suggest that this structure consists of a smaller number of G-quartets. The position of the electrophoretic band also corresponds to the typical signature of a dimeric molecule at 8 °C, but at 40 °C, the position is more characteristic of an unfolded monomeric oligonucleotide. This sequence also contains four cytosines (Cs) that are known to prefer the dimerization of the W−C structure instead of forming a standard G-quadruplex. This aptamer is more stable in the presence of potassium ions, and the CD signal of the molecule is stronger than that of HTR (∼2.7-fold). Two clear conformers were detected using electrophoresis with similar mobilities; these could be topologically different dimers.

The IonK aptamer shows many similarities to HTR, especially in the profile of the CD spectrum, the comparable stability of the molecule, and the R_{Na} and R_K ratios. Some multimerization was also observed in the presence of potassium.

The Insu aptamer demonstrated a high degree of multimerization, and it is possible that the strength of this effect could be affected by the presence of eight neighboring Gs in positions in which a slippage among DNA strands is allowed. A single dimer and a more complex conformer were observed using electrophoresis in the presence of potassium. Although different multimeric forms were detected in the presence of potassium, not all of these can be capable of forming stable G-quadruplexes. Many of these conformers were not observed when electrophoresis was performed at 40 °C. The electrophoretic pattern is similar to the molecular ladder, and the possibility that systematic increases in molecular weight correspond to the formation of G-wire structures cannot be excluded. Interestingly, this ladder was evident even when the DNA sample was loaded in the well a few hours after being heated.

The Scle aptamer forms two intermolecular structures, dimer and tetramer, in the presence of sodium, but only one dimeric structure was detected in the presence of potassium. This aptamer consisted of seven neighboring Gs. The sequences of aptamers EA1D and Scle are very similar, and the two differ by only one nucleotide. The CD spectra and molecularity are also very close in the presence of potassium, but Scle also has an enhanced ability to form tetramolecular structures in the presence of sodium. It is possible to suggest that the exchange of one T for one G renders this aptamer more stable.

The core sequence of the Stat aptamer is the same as that of the EA2D complex, and the two aptamers share almost all of the same biophysical parameters.

Our results concerning parameters R_{Na} and R_K for the TBA aptamer were of particular interest. Previous studies of the TBA structure using NMR had revealed that this aptamer consists of two G-quartets.[45] For such a biquartet molecule, an R_K value of ≈0.5−0.7 is expected, when only the amount of stacking is calculated. Despite the fact that only two G-quartets are present in TBA, the CD signal at 295 nm is comparable with that of the hybrid structure of HTR in the presence of both sodium and potassium. However, our model takes into consideration the configuration of guanines in G-quartets and clearly demonstrates the reason why the peak of TBA at 295 nm reaches an intensity similar to that of HTR, and the ratio is close to 1 (Figure 3). Our results match our hypotheses perfectly, although there is some ambiguity in the position of the electrophoretic band in Figure 4. The mobility of the electrophoretic band in the presence of potassium is lower than that of the larger molecule HTR but higher than that of HIV-93del. This discrepancy may be a result of the different topologies of the HTR and TBA quadruplexes, in terms of both the molecular mass and the shape of molecules. Despite these findings, it is possible to suggest that TBA can also take a dimeric form under certain conditions. It has recently been shown that TBA can be bimolecular under various concentration-dependent salt conditions.[46] Thus, the calculation of R_K was also performed at various concentrations of potassium for all studied oligonucleotides (see also Table S2 of the Supporting Information). However, the R_K value of TBA in the range of 0.4−144 μM in the presence of 50 mM KCl is ∼1. Given that the melting temperature of TBA is 13.5 °C, the position of the aptamer in electrophoresis performed at 40 °C in the presence of sodium is characteristic of an unfolded oligonucleotide. However, there is a significant difference between the mobility levels of TBA in the presence of potassium and in the presence of sodium at 40 °C, which suggests that TBA folds into a G-quadruplex in the presence of potassium. The bands representing stable G-quadruplexes at 40 °C show a slightly higher level of mobility than in the electrophoretic results performed at 8 °C, a finding that is in agreement with previously published results.[18] However, less stable isoforms start to unfold at temperatures below 40 °C, thereby causing a nonlinear change in mobility. This is the case with TBA in sodium buffer and is more evident still for HCV.

Although previous studies have suggested that the TNF aptamer forms a G-quadruplex structure,[35] our results do not appear to support this hypothesis. This aptamer does not fulfill any of the basic criteria for G-quadruplex formation. The CD spectra show no peaks at 265 and 295 nm; the TDS results show no evidence of G-quadruplex formation, and the R_{Na} and R_K ratios are too low. A slight difference in mobility between the molecular standard and the TNF aptamer can be explained by the differing contents of purines and pyrimidines in these two types of DNA.

The apVEGF aptamer and its deleted variant apVEGF-D have the interesting quality of displaying the same melting

temperatures in the presence of sodium as in the presence of potassium; all other known quadruplexes melt at significantly different temperatures in the two buffers. In addition, antiparallel topologies were found to be predominant in the presence of sodium, while parallel structures were favored in the presence of potassium. apVEGF formed a dimeric antiparallel structure in the sodium buffer; however, the population of this conformer was very low, and the conversion of the dimer to an (unfolded) monomer is signified by the smearing of the electrophoretic band during electrophoresis. This effect is similar to that of the Hema aptamer under the same conditions. However, the deleted form, apVEGF-D, formed only a monomeric structure with a similar melting temperature. R_{Na} is 0.9, which indicates that this conformer is a monomer and can be a three-layer quartet G-quadruplex.

Recent studies using NMR have revealed that the apVEGF aptamer folds into unusual topological structures in the presence of potassium ions. First, all five consecutive Gs are involved in G-quartet formation; they occupy the positions in adjacent DNA strands that are bridged with a propeller-type loop without any residue. Second, a two-residue D-shaped loop facilitates the inclusion of an isolated G residue into the vacant spot within the G-quartet. The two remaining G-rich tracts of three residues each adopt a parallel orientation and are linked with edgewise and propeller loops. Finally, both overhangs exhibit well-defined conformations.[47] It is very likely that the first and most intensive band represents this particular structure. However, apVEGF also forms dimeric and higher-order supramolecular conformers, developments that are analogous with those observed for the HIV93del aptamer. An original ^{1}H NMR spectrum showed clear signals in the imino region, which suggests that some W−C hydrogen bonds were formed; indeed, apVEGF does contain 3′ and 5′ overhangs and loop bases that are capable of forming these types of bonds. However, the apVEGF-D sequence forms only a small population of intramolecular conformers, and the dimer and tetramer forms are predominant when the incubation period is longer.

The overhangs in G-quadruplexes have a great influence on their multimerization. The type of ion also influences the topology and molecularity of the final structure, a factor that can also influence the specificity of recognition by a target molecule.

CONCLUSIONS

In this study, a series of simple methods were used to determine the properties of G-rich sequences that have shown potential for the formation of G-quadruplex structures. CD spectroscopy was applied to detect the distinctive signals in wavelength regions that are characteristic of G-quadruplexes, and UV−vis spectroscopy was used to obtain TDS and to determine DNA concentrations for adjustments to the molar dichroism intensity. The intensity of the CD signal was compared with that of the HTR sequence. Standard electrophoresis was also applied to confirm the coexistence of different conformers under given conditions and to estimate the molecularity of these structures. We are aware that the interpretation of CD intensity in relation to molecularity is not straightforward; however, our methodology has been tested on more than 100 other G-quadruplex sequences in addition to the aptamers studied in this work, and no disparities have been found. The methodology was also tested at different concentrations of both sodium and potassium ions, and no discrepancies were observed at concentrations of 25 and 100 mM. In addition, the findings of our studies have been tested against the published work of other authors, and again the results were favorable. In Table S1 of the Supporting Information, calculated parameters of R for other sequences are presented; some of these sequences consist of 5−12 G-runs. These types of sequences have the potential to form tandemic G-quadruplexes,[22] and therefore, the R value is significantly higher; in the case of two-tandemic G-quadruplexes, for example, the value of R for antiparallel G-quadruplexes HTR-HTR approximately doubled in comparison to that of the HTR. On the other hand, G-quadruplexes formed from sequences that consist of fewer than four G-runs must dimerize, and the value of R_K ranges from 0.5 to 1 (e.g., 2G3 and 3G3 in Table S1 of the Supporting Information). Therefore, the comparison of relative CD intensities in the spectral regions characteristic of G-quadruplexes would seem to be a valuable tool in the study of G-quadruplexes. The application of this set of techniques is very simple and cost-efficient and would be highly suitable for use as a preliminary screening method prior to the use of more expensive techniques for determining molecular structure. Our results clearly demonstrate that the CD signal of interlocked G-quadruplex structures in which at least one extra G-quartet is present is higher in comparison to the CD intensity of monomeric isoforms. It is very likely that multimeric and interlocked G-quadruplexes are formed in EA1D, EA2D, EA2aD, HCV, HIV-93del, Hema, Scle, Stat, and vegf sequences in the presence of potassium. Our suggestion is supported by the fact that sequences EA1D, EA2D, EA2aD, and Stat show a very high degree of homology with sequence N-myc (TAG_3-$CG_3AG_3AG_3A_2$). The interlocked nature of the N-myc dimer has been recently confirmed via NMR.[43] However, no significant change in CD intensity was observed in multimeric parallel G-qudruplexes without the formation of extra stacking, e.g., HTR and bcl-2 in PEG 200. An insufficient stacking interaction between two parallel G-quadruplex subunits (usually in a head-to-head interaction) due to longer distances or steric hindrance between G-quartets can result in a failure to observe any new stacking in G-quartet interaction. Despite the dimerization, no additional stacking contribution to the CD signal is observed. Our methodology combined with electrophoresis allows the prediction of interlocked multimeric G-quadruplexes in which new G-quartets are formed.

While at first glance it may appear that the electrophoretic results complicate the interpretation of the data, in fact the opposite is true. The electrophoretic profiles indicate that the coexistence of various forms of G-quadruplexes is a very frequent satellite effect. However, it is important to emphasize a number of details; the process of sample preparation prior to the commencement of electrophoretic separation is a crucial step because the occurrence and formation of some conformers can be affected by the way in which the sample has been prepared. Similarly, the interpretation of TDS is strongly dependent on the stability of the final structure; if the thermal stability of a DNA sample is largely unknown, extreme care should be taken in any interpretation of the obtained data.

ASSOCIATED CONTENT

Supporting Information

Tables S1 and S2 and Figure S1. This material is available free of charge via the Internet at http://pubs.acs.org.

dx.doi.org/10.1021/bi500773c | Biochemistry 2014, 53, 7013−7027

AUTHOR INFORMATION

Corresponding Author

*P. J. Šafárik University, Faculty of Sciences, Institute of Chemistry, Department of Biochemistry, Moyzesova 11, 04011 Košice, Slovakia. Telephone: +421 55 234 12 62. Fax: +421 55 622 21 24. E-mail: viktor.viglasky@upjs.sk.

Funding

This work was supported by the Slovak Research and Development Agency under Contracts APVV-0280-11 and APVV-0134-11 and the Slovak Grant Agency (1/0504/12).

Notes

The authors declare no competing financial interest.

ACKNOWLEDGMENTS

We are grateful to Beate Strehlitz for her valuable comments and information about the EA aptameric sequences. We also thank G. Cowper and L. Sieber for critical reading of the manuscript.

ABBREVIATIONS

CD, circular dichroism; EA, ethanolamine; G-rich, guanine-rich; TDS, thermal difference spectra.

REFERENCES

(1) Cerchia, L., and de Franciscis, V. (2010) Targeting cancer cells with nucleic acid aptamers. *Trends Biotechnol. 28*, 517−525.

(2) Cao, X., Li, S., Chen, L., Ding, H., Xu, H., Huang, Y., Li, J., Liu, N., Cao, W., Zhu, Y., Shen, B., and Shao, N. (2009) Combining use of a panel of ssDNA aptamers in the detection of *Staphylococcus aureus*. *Nucleic Acids Res. 37*, 4621−4628.

(3) Green, L. S., Jellinek, D., Jenison, R., Ostman, A., Heldin, C. H., and Janjic, N. (1996) Inhibitory DNA ligands to platelet-derived growth factor B-chain. *Biochemistry 35*, 14413−14424.

(4) Ruckman, J., Green, L. S., Beeson, J., Waugh, S., Gillette, W. L., Henninger, D. D., Claesson-Welsh, L., and Janjic, N. (1998) 2′-Fluoropyrimidine RNA-based aptamers to the 165-amino acid form of vascular endothelial growth factor (VEGF165). Inhibition of receptor binding and VEGF-induced vascular permeability through interactions requiring the exon 7-encoded domain. *J. Biol. Chem. 273*, 20556−20567.

(5) Choi, E. W., Nayak, L. V., and Bates, P. J. (2010) Cancer-selective antiproliferative activity is a general property of some G-rich oligodeoxynucleotides. *Nucleic Acids Res. 38*, 1623−1635.

(6) Cao, Z., Huang, C. C., and Tan, W. (2006) Nuclease resistance of telomere-like oligonucleotides monitored in live cells by fluorescence anisotropy imaging. *Anal. Chem. 78*, 1478−1484.

(7) Víglaský, V., and Hianik, T. (2013) Potential uses of G-quadruplex-forming aptamers. *Gen. Physiol. Biophys. 32*, 149−172.

(8) Tucker, W. O., Shum, K. T., and Tanner, J. A. (2012) G-quadruplex DNA aptamers and their ligands: Structure, function and application. *Curr. Pharm. Des. 18*, 2014−2026.

(9) Tsukakoshi, K., Abe, K., Sode, K., and Ikebukuro, K. (2012) Selection of DNA aptamers that recognize α-synuclein oligomers using a competitive screening method. *Anal. Chem. 84*, 5542−5547.

(10) Gatto, B., Palumbo, M., and Sissi, C. (2009) Nucleic acid aptamers based on the G-quadruplex structure: Therapeutic and diagnostic potential. *Curr. Med. Chem. 16*, 1248−1265.

(11) Yoshida, W., Saito, T., Yokoyama, T., Ferri, S., and Ikebukuro, K. (2013) Aptamer selection based on g4-forming promoter region. *PLoS One 8*, e65497.

(12) Agrawal, P., Hatzakis, E., Guo, K., Carver, M., and Yang, D. (2013) Solution structure of the major G-quadruplex formed in the human VEGF promoter in K^+: Insights into loop interactions of the parallel G-quadruplexes. *Nucleic Acids Res. 41*, 10584−10592.

(13) Dai, J., Chen, D., Jones, R. A., Hurley, L. H., and Yang, D. (2006) NMR solution structure of the major G-quadruplex structure formed in the human BCL2 promoter region. *Nucleic Acids Res. 34*, 5133−5144.

(14) Dai, J., Dexheimer, T. S., Chen, D., Carver, M., Ambrus, A., Jones, R. A., and Yang, D. (2006) An intramolecular G-quadruplex structure with mixed parallel/antiparallel G-strands formed in the human BCL-2 promoter region in solution. *J. Am. Chem. Soc. 128*, 1096−1098.

(15) Phan, A. T., Kuryavyi, V., Burge, S., Neidle, S., and Patel, D. J. (2007) Structure of an unprecedented G-quadruplex scaffold in the human c-kit promoter. *J. Am. Chem. Soc. 129*, 4386−4392.

(16) Phan, A. T., Modi, Y. S., and Patel, D. J. (2004) Propeller-type parallel-stranded G-quadruplexes in the human c-myc promoter. *J. Am. Chem. Soc. 126*, 8710−8716.

(17) Ambrus, A., Chen, D., Dai, J., Jones, R. A., and Yang, D. (2005) Solution structure of the biologically relevant G-quadruplex element in the human c-MYC promoter. Implications for G-quadruplex stabilization. *Biochemistry 44*, 2048−2058.

(18) Víglaský, V., Bauer, L., and Tlučková, K. (2010) Structural features of intra- and intermolecular G-quadruplexes derived from telomeric repeats. *Biochemistry 49*, 2110−2120.

(19) Mann, D., Reinemann, C., Stoltenburg, R., and Strehlitz, B. (2005) In vitro selection of DNA aptamers binding ethanolamine. *Biochem. Biophys. Res. Commun. 338*, 1928−1934.

(20) Reinemann, C., Stoltenburg, R., and Strehlitz, B. (2009) Investigations on the specificity of DNA aptamers binding to ethanolamine. *Anal. Chem. 81*, 3973−3978.

(21) Tlučková, K., Marušič, M., Tóthová, P., Bauer, L., Šket, P., Plavec, J., and Víglaský, V. (2013) Human papillomavirus G-quadruplexes. *Biochemistry 52*, 7207−7216.

(22) Bauer, L., Tlučková, K., Tóthová, P., and Víglaský, V. (2011) G-quadruplex motifs arranged in tandem occurring in telomeric repeats and the insulin-linked polymorphic region. *Biochemistry 50*, 7484−7492.

(23) Mergny, J. L., Li, J., Lacroix, L., Amrane, S., and Chaires, J. B. (2005) Thermal difference spectra: A specific signature for nucleic acid structures. *Nucleic Acids Res. 33*, e138.

(24) Gray, D. M., Wen, J. D., Gray, C. W., Repges, R., Repges, C., Raabe, G., and Fleischhauer, J. (2008) Measured and calculated CD spectra of G-quartets stacked with the same or opposite polarities. *Chirality 20*, 431−440.

(25) Karsisiotis, A. I., Hessari, N. M., Novellino, E., Spada, G. P., Randazzo, A., and Webba da Silva, M. (2011) Topological characterization of nucleic acid G-quadruplexes by UV absorption and circular dichroism. *Angew. Chem., Int. Ed. 50*, 10645−10648.

(26) Karsisiotis, A. I., O'Kane, C., and Webba da Silva, M. (2013) DNA quadruplex folding formalism: A tutorial on quadruplex topologies. *Methods 64*, 28−35.

(27) Masiero, S., Trotta, R., Pieraccini, S., De Tito, S., Perone, R., Randazzo, A., and Spada, G. P. (2010) A non-empirical chromophoric interpretation of CD spectra of DNA G-quadruplex structures. *Org. Biomol. Chem. 8*, 2683−2692.

(28) Vorlíčková, M., Kejnovská, I., Bednářová, K., Renčiuk, D., and Kypr, J. (2012) Circular dichroism spectroscopy of DNA: From duplexes to quadruplexes. *Chirality 24*, 691−698.

(29) Luu, K. N., Phan, A. T., Kuryavyi, V., Lacroix, L., and Patel, D. J. (2006) Structure of the human telomere in K^+ solution: An intramolecular (3 + 1) G-quadruplex scaffold. *J. Am. Chem. Soc. 128*, 9963−9970.

(30) Ambrus, A., Chen, D., Dai, J., Bialis, T., Jones, R. A., and Yang, D. (2006) Human telomeric sequence forms a hybrid-type intramolecular G-quadruplex structure with mixed parallel/antiparallel strands in potassium solution. *Nucleic Acids Res. 34*, 2723−2735.

(31) Buscaglia, R., Miller, M. C., Dean, W. L., Gray, R. D., Lane, A. N., Trent, J. O., and Chaires, J. B. (2013) Polyethylene glycol binding alters human telomere G-quadruplex structure by conformational selection. *Nucleic Acids Res. 41*, 7934−7946.

(32) Kejnovská, I., Vorlíčková, M., Brázdová, M., and Sagi, J. (2014) Stability of human telomere quadruplexes at high DNA concentrations. *Biopolymers 101*, 428−438.

(33) Víglaský, V., Tlučková, K., and Bauer, L. (2011) The first derivative of a function of circular dichroism spectra: Biophysical study of human telomeric G-quadruplex. *Eur. Biophys. J. 40*, 29−37.
(34) Phan, A. T., Kuryavyi, V., Ma, J. B., Faure, A., Andréola, M. L., and Patel, D. J. (2005) An interlocked dimeric parallel-stranded DNA quadruplex: A potent inhibitor of HIV-1 integrase. *Proc. Natl. Acad. Sci. U.S.A. 102*, 634−639.
(35) Orava, E. W., Jarvik, N., Shek, Y. L., Sidhu, S. S., and Gariepy, J. (2013) A short DNA aptamer that recognizes TNF-α and blocks its activity in vitro. *ACS Chem. Biol. 8*, 170−178.
(36) Víglaský, V., Bauer, L., Tlučková, K., and Javorský, P. (2010) Evaluation of human telomeric G-quadruplexes: The influence of overhanging sequences on quadruplex stability and folding. *J. Nucleic Acids*, No. 820356.
(37) Mukundan, V. T., and Phan, A. T. (2013) Bulges in G-Quadruplexes: Broadening the Definition of G-Quadruplex-Forming Sequences. *J. Am. Chem. Soc. 135*, 5017−5028.
(38) Do, N. Q., Lim, K. W., Teo, M. H., Heddi, B., and Phan, A. T. (2011) Stacking of G-quadruplexes: NMR structure of a G-rich oligonucleotide with potential anti-HIV and anticancer activity. *Nucleic Acids Res. 39*, 9448−9457.
(39) Mukundan, V. T., Do, N. Q., and Phan, A. T. (2011) HIV-1 integrase inhibitor T30177 forms a stacked dimeric G-quadruplex structure containing bulges. *Nucleic Acids Res. 39*, 8984−8991.
(40) Cheng, X., Liu, X., Bing, T., Zhao, R., Xiong, S., and Shangguan, D. (2009) Specific DNA G-quadruplexes bind to ethanolamines. *Biopolymers 91*, 874−883.
(41) Kuryavyi, V., Phan, A. T., and Patel, D. J. (2010) Solution structures of all parallel-stranded monomeric and dimeric G-quadruplex scaffolds of the human c-kit2 promoter. *Nucleic Acids Res. 38*, 6757−6773.
(42) Kuryavyi, V., Cahoon, L. A., Seifert, H. S., and Patel, D. J. (2012) RecA-binding pilE G4 sequence essential for pilin antigenic variation forms monomeric and 5′ end-stacked dimeric parallel G-quadruplexes. *Structure 20*, 2090−2102.
(43) Trajkovski, M., Webba da Silva, M., and Plavec, J. (2012) Unique structural features of interconverting monomeric and dimeric G-quadruplexes adopted by a sequence from the intron of the N-myc gene. *J. Am. Chem. Soc. 134*, 4132−4141.
(44) Ilc, T., Šket, P., Plavec, J., Webba da Silva, M., Drevenšek-Olenik, I., and Spindler, L. (2013) Formation of G-Wires: The Role of G:C-Base Pairing and G-Quartet Stacking. *J. Phys. Chem. C 117*, 23208−23215.
(45) Macaya, R. F., Schultze, P., Smith, F. W., Roe, J. A., and Feigon, J. (1993) Thrombin-binding DNA aptamer forms a unimolecular quadruplex structure in solution. *Proc. Natl. Acad. Sci. U.S.A. 90*, 3745−3749.
(46) Fialová, M., Kypr, J., and Vorlícková, M. (2006) The thrombin binding aptamer GGTTGGTGTGGTTGG forms a bimolecular guanine tetraplex. *Biochem. Biophys. Res. Commun. 344*, 50−54.
(47) Marušič, M., Veedu, R. N., Wengel, J., and Plavec, J. (2013) G-rich VEGF aptamer with locked and unlocked nucleic acid modifications exhibits a unique G-quadruplex fold. *Nucleic Acids Res. 41*, 9524−9536.
(48) Jones, L. A., Clancy, L. E., Rawlinson, W. D., and White, P. A. (2006) High-affinity aptamers to subtype 3a hepatitis C virus polymerase display genotypic specificity. *Antimicrob. Agents Chemother. 50*, 3019−3027.
(49) Jing, N., and Hogan, M. E. (1998) Structure-activity of tetrad-forming oligonucleotides as a potent anti-HIV therapeutic drug. *J. Biol. Chem. 273*, 34992−34999.
(50) Okazawa, A., Maeda, H., Fukusaki, E., Katakura, Y., and Kobayashi, A. (2000) In vitro selection of hematoporphyrin binding DNA aptamers. *Bioorg. Med. Chem. Lett. 10*, 2653−2656.
(51) Li, Y., Geyer, C. R., and Sen, D. (1996) Recognition of anionic porphyrins by DNA aptamers. *Biochemistry 35*, 6911−6922.
(52) Yoshida, W., Mochizuki, E., Takase, M., Hasegawa, H., Morita, Y., Yamazaki, H., Sode, K., and Ikebukuro, K. (2009) Selection of DNA aptamers against insulin and construction of an aptameric enzyme subunit for insulin sensing. *Biosens. Bioelectron. 24*, 1116−1120.
(53) Ueyama, H., Takagi, M., and Takenaka, S. (2002) A novel potassium sensing in aqueous media with a synthetic oligonucleotide derivative. Fluorescence resonance energy transfer associated with guanine quartet-potassium ion complex formation. *J. Am. Chem. Soc. 124*, 14286−14287.
(54) Shum, K. T., Chan, C., Leung, C. M., and Tanner, J. A. (2011) Identification of a DNA aptamer that inhibits sclerostin's antagonistic effect on Wnt signalling. *Biochem. J. 434*, 493−501.
(55) Zhu, Q., and Jing, N. (2007) Computational study on mechanism of G-quartet oligonucleotide T40214 selectively targeting Stat3. *J. Comput.-Aided Mol. Des. 21*, 641−648.
(56) Schultze, P., Macaya, R. F., and Feigon, J. (1994) Three-dimensional solution structure of the thrombin-binding DNA aptamer d(GGTTGGTGTGGTTGG). *J. Mol. Biol. 235*, 1532−1547.
(57) Nonaka, Y., Sode, K., and Ikebukuro, K. (2010) Screening and improvement of an anti-VEGF DNA aptamer. *Molecules 15*, 215−225.